

Normal state Raman spectra of high- T_c cuprates

K C Bishoyi^{1*}, G C Rout² and S N Behera³

¹P G Department of Physics, F M College (Autonomous), Balasore-756 001, Orissa, India

²Condensed Matter Physics Group, Govt Science College, Chatrapur-761 020, Orissa, India

³Institute of Physics, Sachivalaya Marg, Bhubaneswar-751 005, Orissa, India

E-mail: bishoyi@iopb.res.in

Abstract : We present a microscopic theory to explain Raman spectra of high- T_c cuprates $R_{2-x}M_xCuO_4$ in the normal state. We used electronic Hamiltonian prescribed by Fulde in presence of anti-ferromagnetism. Phonon interaction to the hybridization between the conduction electrons of the system and the f -electrons has been incorporated in the calculation. The phonon spectral density is calculated by the Green function technique of Zubarev at zero wave vector and finite (room) temperature limit. Parameter dependence of Raman active phonon frequencies are studied by varying model parameters of the system *i.e.* the position of f -level (ϵ_f), the effective electron-phonon coupling strength (g), the staggered magnetic field (h_1), and the hybridization parameter (v). The four Raman active peaks (P_1 to P_4) represent the electronic states of the atomic sub-systems of the cuprate systems. They show up as phonon excitations due to the coupling of the phonon to the electrons and the anti-ferromagnetic gap

Keywords : Anti-ferromagnetic order, electron-phonon interaction, Raman scattering.

PACS Nos. : 71.38.+i, 78.30.-j

1. Introduction

Recently, a detailed study of Raman measurements on cuprate systems ($R_{2-x}Ce_xCuO_4$; $R = Pr, Nd, Sm, Gd$) in the normal and the superconducting states have been reported [1]. The Raman data of $R_{2-x}Ce_xCuO_4$ shows several peaks due to deliverance of phonons of different origin over the constant intensity background [2]. These peaks show anomalous evolution of the peak structure with temperature and doping. Raman investigations of $Nd_{2-x}Ce_xCuO_4$ [3] as well as some of the infrared reflectivity [4] focused on symmetry determination and the assignments of the $A_{1g} + B_{1g} + 2E_g$ Raman active and $3A_{2u} + 4E_u$ infrared active phonons. Such assignments were confirmed with the help of lattice dynamical calculations. Four Raman active phonons for Nd_2CuO_4 (D_{4h}^{17})(I_4/mmm space group) are $A_{1g} + B_{1g} + 2E_g$. Three of these modes have clearly been assigned. These three frequencies are A_{1g} (229 cm^{-1}) due to Nd vibration, B_{1g} (342 cm^{-1}) due to out of plane oxygen vibration and E_g (489 cm^{-1}) due to in-plane oxygen vibration. The fourth frequency of E_g (122 cm^{-1}) mode of Nd at room temperature for $Nd_{2-x}Ce_xCuO_4$ ($x = 0.15$) is

controversial [5]. Short communications have been reported on theoretical investigations of velocity of sound [6] and Raman spectra [7-9] of the cuprate systems. Recently, we have reported the studies on phonon dispersion in the static limit [10], temperature dependence of phonon frequency [11] and ultrasonic attenuation [12] in the normal state in cuprate systems. In our present communication, we address parameter dependence of the Raman spectra of the cuprate system in normal state at room temperature.

2. Formalism

Simulating the strong electron in the CuO plane by breaking the spin symmetry, the heavy fermion behaviour of $Nd_{2-x}Ce_xCuO_4$ ($x = 0.2$) can be understood. The starting point is a lattice Hamiltonian which includes effective Nd-Cu hybridization which is mediated by oxygen ions. Having to deal thereby with three strongly correlated f -electrons for Nd is a problem in itself. To avoid it, Fulde has considered only one orbital per Nd ion. This is reasonable since the crystal field ground state is a doublet [13]. The

*Corresponding Author

large on site Coulomb interaction between Cu 3d electrons suppresses almost all the configurations with empty $d_{x^2-y^2}$ orbitals and result in the anti-ferromagnetic correlation between different copper sites. It is well known that anti-ferromagnetic correlation can be simulated well by a spin symmetry break up. Therefore, we work here with an anti-ferromagnetic ground state, although long range AF order is destroyed in $\text{Nd}_{1.8}\text{Ce}_{0.2}\text{CuO}_4$ due to electron doping. It is emphasized that symmetry breaking is used only for modeling the strong correlation. By doing so charge fluctuation among electrons in the copper oxide planes are strongly reduced *via* the Cu-Nd interactions of f -electrons on Nd sites. This model can explain the heavy fermion-like behaviour of $\text{Nd}_{1.8}\text{Ce}_{0.2}\text{CuO}_4$. the above experimental results are explained by a model given by Fulde [14].

The Hamiltonian in k -space for the cuprate system is taken as

$$\mathcal{H}_0 = \mathcal{H}_d + \mathcal{H}_s + \mathcal{H}_v + \mathcal{H}_f, \quad (1)$$

where

$$\mathcal{H}_d = \sum_{k,\sigma} \epsilon_0(k) (a_{k,\sigma}^\dagger b_{k,\sigma} + h.c) \quad (2)$$

with dispersion $\epsilon_0(k) = -2$ to $(\cos k_x + \cos k_y)$.

$$\mathcal{H}_s = (h/2) \sum_{k,\sigma} \sigma (a_{k,\sigma}^\dagger a_{k,\sigma} - a_{k,\sigma}^\dagger a_{k,\sigma}), \quad (3)$$

$$\mathcal{H}_v = V \sum_{k,\sigma} (a_{k,\sigma}^\dagger f_{1,k,\sigma} + a_{k,\sigma}^\dagger f_{1,k,\sigma} + h.c), \quad (4)$$

$$\mathcal{H}_f = \epsilon_f \sum_{k,\sigma} f_{1,k,\sigma}^\dagger f_{1,k,\sigma}. \quad (5)$$

\mathcal{H}_d , \mathcal{H}_s , \mathcal{H}_v and \mathcal{H}_f are conduction electron, staggered field, hybridization interaction and f -electron Hamiltonian respectively. Here a^\dagger (a), b^\dagger (b) are creation (annihilation) operators for the $d_{x^2-y^2}$ conduction electrons on copper sub-lattices 1 and 2 respectively and f^\dagger (f) are those for the f -electrons. The Fourier transformed electron-phonon interaction Hamiltonian is

$$\begin{aligned} \mathcal{H}_{e-p} = \sum_{k,q,\sigma} f(q) [(a_{k+q,\sigma}^\dagger f_{1,k,\sigma} + b_{k+q,\sigma}^\dagger f_{1,k,\sigma}) \\ + h.c.] A_q \end{aligned} \quad (6)$$

with $h.c. = (f_{1,k+q,\sigma}^\dagger a_{k,\sigma} + f_{1,k+q,\sigma}^\dagger b_{k,\sigma})$ and $A_q = b_q + b_{-q}^\dagger$,

where b_q (b_q^\dagger) are annihilation (creation) operators for phonon with wave vector q and $f(q)$ is the electron-phonon coupling constant. The free phonon Hamiltonian with phonon energy ω_q is written as $\mathcal{H}_p = \sum_q \omega_q b_q^\dagger b_q$. Hence, the total Hamiltonian of the system is described by

(7)

The double time phonon Green function of Zubarev [15] type is defined as

$$\begin{aligned} D_{q,q}(t-t') = << A_q(t); A_q(t') >> \\ = -i\Theta(t-t') <[A_q(t); A_q(t')]>. \end{aligned} \quad (8)$$

Applying Dyson approximation, the phonon Green function can be written as

$$D_{q,q}(\omega) = (\omega_q / \pi) [\omega^2 - \omega_q^2 - \sum_q(\omega)]^{-1}, \quad (9)$$

where phonon self energy is given by

$$\sum_q(\omega) = 4\pi f^2(-q) \omega_q \chi_{qq}(\omega), \quad (10)$$

$$\chi_{q,q'}(\omega) = \sum_{k,k',\sigma,\sigma'} [\Gamma_3 + \Gamma_4 + \Gamma_5 + \Gamma_6 +], \quad (11)$$

$\Gamma_i(k,k',q,q',\omega)$'s ($i = 3$ to 6) represent the electron response functions. They are defined by dropping k,k',q,q' and ω as

$$\begin{aligned} \Gamma_3(\omega) &= << \alpha^a + \alpha^b, \beta^a >>; \\ \Gamma_4(\omega) &= << \alpha^a + \alpha^b, \beta^b >>; \\ \Gamma_5(\omega) &= << \alpha^c + \alpha^d, \beta^a >>; \\ \Gamma_6(\omega) &= << \alpha^c + \alpha^d, \beta^b >>; \end{aligned} \quad (12)$$

where

$$\begin{aligned} \alpha^a &= a_{k-q,\sigma}^\dagger f_{k,\sigma}; \quad \alpha^b = f_{k-q,\sigma}^\dagger a_{k,\sigma}; \\ \alpha^c &= b_{k-q,\sigma}^\dagger f_{k,\sigma}; \quad \alpha^d = f_{k-q,\sigma}^\dagger b_{k,\sigma}; \end{aligned} \quad (13)$$

$$\begin{aligned} \beta^a &= a_{k'-q',\sigma}^\dagger f_{k',\sigma'} + f_{k'-q',\sigma}^\dagger a_{k',\sigma'}; \\ \beta^b &= b_{k'-q',\sigma}^\dagger f_{k',\sigma'} + f_{k'-q',\sigma}^\dagger b_{k',\sigma'}. \end{aligned} \quad (14)$$

We make some approximations, while calculating the electron

response function, keeping the essential physics intact. We use certain decoupling schemes for the higher order Green's functions such that all the physical parameters like f -level, staggered magnetic field, hybridization term ($\sim V^2$) and phonon coupling term are retained. The limit of zero wave vector ($q \rightarrow 0$) and finite temperature are considered in evaluating the response function.

4. Expression for phonon spectral density

Here, we are interested to explain the observed Raman intensity due to contribution of phonon only. Hence, we calculate phonon spectral density function $S(q=0, \omega) = -\text{Im}.D_{qq}(q=0, \omega)$, where $D_{qq}(0, \omega)$ is the phonon Green function for $q=0$. The self energy of the phonon being proportional to the density response function $S(0, \omega)$, will reflect the properties of ground state of the cuprates in normal state. Since in light scattering the momentum conservation requires only, the $q=0$ process, it is the zone centre optic phonon which will couple to the electron number operator of conduction electrons, f -electrons and the modulation of f - and c -electrons. The phonon self energy depends on different model parameters through the electron response function $\chi_{00}(\omega)$. In order to compare the theoretical calculations with the experimental results, we need to calculate the spectral density function $S(0, \omega)$, which is the quantity one measures in Raman scattering. The $S(0, \omega)$ is calculated by attributing a finite width (η) to the phonon frequency ($\omega^2 \rightarrow \omega^2 + 2i\omega\eta$). The results of the phonon self energy show up as the peaks in the spectral density function.

The spectral density function is written as

$$S(\omega, \omega) = \frac{2\omega_n^2 B_1}{A_1^2 + B_1^2}, \quad (15)$$

where

$$A_1 = [\omega^2 - \omega_0^2(1 + 4A_2)],$$

$$B_1 = [2\eta\omega - 4g\omega_0^2 B_2],$$

A_2 and B_2 are written as

$$A_2 = g \int_{-W/2}^{W/2} dx_0 A_3(\epsilon_k, \omega),$$

$$B_2 = g \int_{-W/2}^{W/2} dx_0 B_3(\epsilon_k, \omega), \quad (16)$$

where

$$A_3(\epsilon_k, \omega) = \frac{1}{D_{12}} [A_6 P_1 f(\omega_1) + A_7 Q_1 f(\omega_2) + A_8 R_1 f(\omega_3)],$$

$$B_3(\epsilon_k, \omega) = \frac{1}{D_{12}} [B_6 P_1 f(\omega_1) + B_7 Q_1 f(\omega_2) + B_8 R_1 f(\omega_3)].$$

$A_6, A_7, A_8, B_6, B_7, B_8, D_{12}, P_1, Q_1$ and R_1 are expressed in terms of other known dimensionless parameters. Here, $f(\omega_i)$ are the fermi functions which are in turn with $i=1$ to 3. Different parameters used in the above expressions are made dimensionless by dividing them by hopping integral $2t_0$, where the width of the conduction band is $W=8t_0$. Those are

$$g = f^2(0) N(0)/\omega_0, \quad d = \epsilon_f/2t_0, \quad c = \omega/2t_0,$$

$$v = V/2t_0, \quad e = \eta/2t_0, \quad p = \omega_0/2t_0,$$

$$\tilde{\omega} = c/p, \quad x_0 = \epsilon_0/2t_0, \quad h_1 = h/2t_0,$$

$$t = k_B T/2t_0,$$

where k_B is the Boltzmann constant. And other variables are

$$x = \{x_0^2 + (h^2/4)\}^{1/2}, \quad \tilde{\Delta} = [(x-d)^2 + 8v^2]^{1/2},$$

$$\omega = \lambda_0, \quad \tilde{\omega}_{2,3} = (x + d \pm \tilde{\Delta})/2. \quad (17)$$

5. Results and discussion

In the present model, it is predominantly the coupling of the phonon to hybridization, while in Balseiro-Falicov (BF) [16] model of Charge density wave superconductivity (CDW-SC), the phonon is coupled to the conduction electron. This is somewhat analogous to the observation of a superconducting excitation peak through the coupling of SC to CDW amplitude phonons by Sooryakumar and Klein [17,18]. In extending the BF model to calculate the small wave vector (q) dependent phonon self energy, Mohanty and Behera [19] have predicted an additional low frequency mode besides gap excitation mode to be present in the $q=0$ limit. The present model considers anti-ferromagnetic ground state in presence of a weak hybridization between the f -electrons of the rare-earth atom and conduction electrons of the copper atoms. Here in this case, the AFM excitation gap is expected to be manifested through its coupling to the phonon in the phonon spectral density function. The collective mode of the magnetic excitation state should also appear in the Raman spectrum

analogous to the CDW amplitude mode of the CDW-superconducting state. Earlier Rout *et al* [8] have reported the results of Raman spectra of cuprate superconductors in the high temperature range ($T > 450$ K) in the light of the present model. Therefore, they have considered a weak electron-phonon coupling constant $g = 6 \times 10^{-9}$. Here we report Raman spectra of the cuprates at room temperature below the Néel temperature ($T_N \simeq 250$ K) which is the

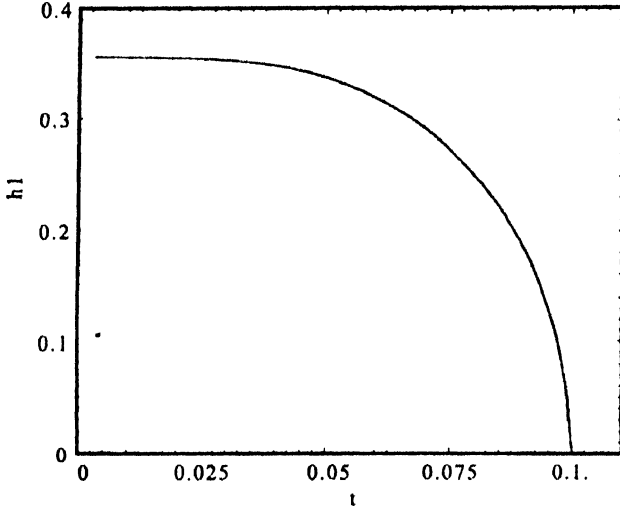


Figure 1. The plots of $h1$ vs t for fixed values of $d = 0.06$, $v = 0.015$, $\lambda_2 = 0.320522$.

experimentally observed transition temperature [13]. Different dimensionless parameters involved in the numerical calculations are the effective coupling strength of phonon with the hybridization (g), the position of the renormalised f -level (d), hybridization matrix element (V), staggered magnetic field strength parameter ($h1$), the renormalized phonon frequency parameter (c) and the temperature parameter ($t = k_B T / 2t_0$). These parameters influence the spectral density function of the cuprate superconductors.

The Figure 1 shows the temperature dependence of the staggered field $h1$ corresponding to the Néel temperature $t_N \simeq 0.1$ ($T_N \simeq 250$ K), $h1(T = 0) \simeq 0.34$ and anti-ferromagnetic (AFM) coupling strength $\lambda_2 = 0.320522$. This represents well the normal AFM state of the cuprate system [13]. From this plot, we have chosen bare $h1 \simeq 0.95$ at temperature $t = 0.09$. We want to study normal state Raman spectra at $t \simeq 0.09$ ($T \simeq 225$) with weak hybridization $v = 0.015$ and f -level position $d = 0.06$ *i.e.* close to Fermi level.

From the temperature variation of phonon frequency in normal state of cuprates we have fixed the phonon parameters *i.e.* phonon coupling strength $g \simeq 0.025$ [11], bare phonon frequency $p \simeq 1.0$ and the phonon life-time broadening parameter $e \simeq 0.018$. It is commonly believed that the electron-phonon interaction is very weak in high T_c copper

oxide superconductors. A very weak electron-phonon coupling of $g = 6 \times 10^{-9}$ in copper oxide superconductors at high temperatures has been rightly reported [8]. But the

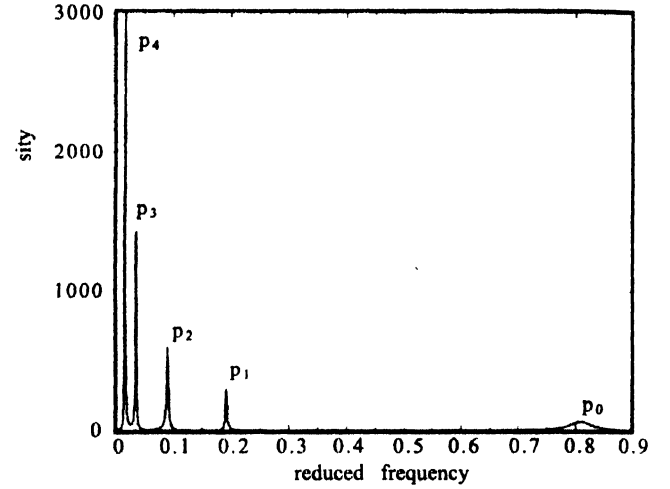


Figure 2. The plot of spectral density function vs reduced frequency for fixed values of $e = 0.018$, $p = 1.0$, $t = 0.09$, $g = 0.025$, $d = 0.06$, $v = 0.015$, $h1 = 0.195$.

value of this coupling is much smaller compared to that in case of CDW phase superconductors ($g = 0.11$ to 0.15) [16,19]. The value of g is equal to 0.025 in the present case which is seemingly appropriate for the high- T_c systems in non-superconducting magnetic phase at room temperature. A phonon coupling constant $g \simeq 0.0252$ is observed for heavy fermion systems worked out in the framework of periodic Anderson model [20].

In Figure 2 the phonon spectral density function (SDF) is plotted against the reduced phonon frequency $\tilde{\omega} (= \omega/\omega_0)$ for fixed values of d , v , $h1$, g , p , e , and t for normal state of the cuprate systems. Here, we observe five peaks. The peak centered at $\tilde{\omega} \simeq 0.81$ is denoted as P_0 and it corresponds to the renormalized bare phonon frequency of the cuprate systems for $q = 0$ phonon. The other four peaks centered at frequencies $\tilde{\omega} \simeq 0.193$, 0.09 , 0.036 and 0.016 are denoted as P_1 , P_2 , P_3 and P_4 . In absence of electron-phonon coupling ($g = 0$), the phonon self energy is zero. Hence, we observe the phonon peak P_0 at frequency $\tilde{\omega} = 1$ which corresponds to bare phonon frequency ω_q at $q = 0$. When the phonon coupling g is increased, the phonon self energy increases and hence it renormalises the phonon frequency. As a result the phonon frequency decreases and the peak P_0 shifts to lower frequencies and appears at $\tilde{\omega} = 0.81$. The other excitation peaks (P_1 to P_4) appear in the phonon spectrum corresponding to the phonon self energy with appropriate phonon coupling $g = 0.025$. These excitation peaks disap-

peak for g value relatively smaller or relatively larger than $g = 0.025$.

The excitation peaks P_1 to P_4 are identified as follows. In the absence of f -level ($d = 0$) and hybridization ($\nu = 0$), there appears a peak at $\tilde{\omega} \approx 0.193$. This value of energy is very nearly equal to the bare AFM staggered field at temperature $t = 0.09$ ($T = 225$ K) in absence of electron-phonon interaction. The staggered field is slightly reduced due to the electron-phonon interaction; so the peak P_1 centered at the renormalised phonon frequency $\tilde{\omega} \approx 0.193$ is due to the AFM excitation gap. In absence of AFM field ($h_1 = 0$), peak P_2 appears at $\tilde{\omega} \approx 0.09$. Moreover when the hybridization $\nu = 0$, the peak P_2 appears at $\tilde{\omega} \approx 0.09$ in addition to peak P_1 at $\tilde{\omega} \approx 0.193$. Hence the peak P_2 is assigned to be the excitation peak due to the f -level. The f -level position is originally placed at $d = 0.06$ above the Fermi level ($\epsilon_F = 0$). However due to electron-phonon interaction and the presence of AFM in the system the f -

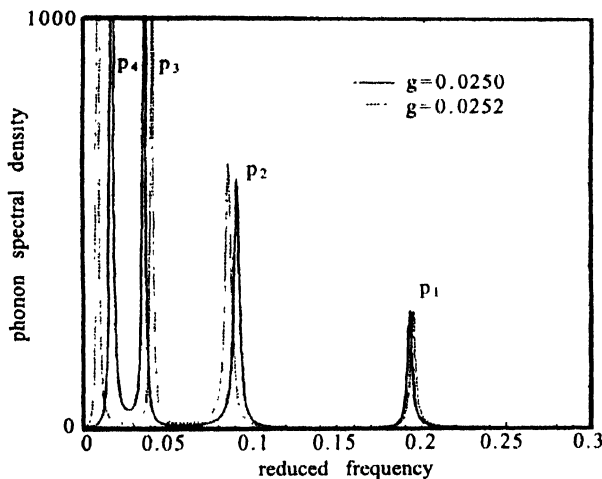


Figure 3. The plot of spectral density function vs reduced frequency for fixed values of $e = 0.018$, $p = 1.0$, $t = 0.09$, $d = 0.06$, $\nu = 0.015$, $h_1 = 0.195$ and for different values of $g = 0.0250, 0.0252$.

level is renormalised and shifted to the position $\tilde{\omega} \approx 0.09$. This peak P_2 appears in the Raman spectra as the AFM excited d -level.

The peaks P_3 and P_4 are quasi-particle bands with P_3 bearing the conduction band character in which AFM exists and P_4 bearing f -electron character. These bands are renormalized and appear due to AFM gap excitation. The peaks P_3 and P_4 are split peaks due to hybridization ν .

The electron-phonon coupling $g \approx 0.0250$ influences all the four peaks as observed in Figure 3. the peaks P_1 and P_3 , with more AFM character, shift to the higher frequencies (harden) but the peaks P_2 and P_4 , having f -electron

character, shift to lower frequencies (soften). In the extreme limits, the excitation of the four peaks appear for the electron phonon coupling $0.018 \leq g \leq 0.026$.

When the f -level of the rare-earth atom lies below the Fermi level (ϵ_F) (i.e. $d = -0.06$), only one peak is observed at $\tilde{\omega} = 0.225$ in addition to phonon peak P_0 at $\tilde{\omega} = 0.093$ for the same electron-phonon coupling constant $g = 0.025$ (not shown in the Figure). For similar electron phonon coupling, the renormalised phonon peak shifts to higher frequencies for $d = -0.06$ compared to that for $d = +0.06$. In addition to this, the AFM peak is renormalised to the higher value $\tilde{\omega} = 0.225$ for $d = -0.06$ unlike the case for $d = +0.06$ where the AFM peak appears at $\tilde{\omega} \approx 0.193$ for the same value of $g (= 0.025)$.

6. Conclusion

We studied temperature variation of phonon frequency in normal state of cuprates to fix the phonon parameters i.e. phonon coupling strength g and bare phonon frequency p and phonon life-time broadening parameter e . For a set of fixed values of d , ν , h_1 , g , p , e and t we observed five peaks and identified those peaks. The effect of variation of g on different peaks are studied which provides much information regarding role of phonon coupling in the presence of AFM for the occurrence of peaks. We wish to vary the other parameters like d , ν , e , p and t and to study the nature of peaks later. The results thus obtained will be reported elsewhere.

Acknowledgments

The authors (KCB and GCR) would like to thank the UGC, New Delhi for providing financial assistance vide letter No : F-PSO-35/98-99(ERO) dated : 25.2.1999. They gratefully acknowledge the research facilities offered by the Institute of Physics, Bhubaneswar, Orissa, India.

References

- [1] E T Heyen, R Liu, M Cardona, S Pinol, R J Melville, D Mck Paul, E Moran and M A Alario-Franco *Phys. Rev.* **B43** 2857 (1990)
- [2] K L Pokhodnia *et al.*, *Z. Phys.* **90** 275 (1993)
- [3] V M Orera, M L Sanjuan, R Alcalá, J Fontcuberta and S Pinol *Physica C* **168** 161 (1990)
- [4] M K Crawford, G Burns, G V Chandrasekhar, F H Daol, W F Farnth, E M McCarron and R J Smalley *Phys. Rev.* **B41** 8933 (1990)
- [5] S Jandl, M Ilive, C Thomson, T Ruf and M Cardona *Solid State Commun.* **87** 609 (1996)
- [6] G C Rout, B N Panda and S N Bchera *Solid State Commun.* **105** 47 (1998)

- [7] B N Panda, G C Rout and S N Behera *Solid State Commun.* **106** 469 (1998)
- [8] G C Rout, B N Panda and S N Behera *Physica* **B271** 136 (1999)
- [9] B N Panda, G C Rout and S N Behra *Int. J. Mod. Phys.* **13(3)** 293 (1999)
- [10] K C Bishoyi, G C Rout and S N Behera *Indian J. Phys.* **75A** 17 (2001)
- [11] K C Bishoyi, G C Rout and S N Behera *Indian J. Phys.* **76A** 87 (2002)
- [12] K C Bishoyi, G C Rout and S N Behera *Proc. DAESSPS* (2000); (G. G. University, Bilaspur. S. S. Physics, India) Vol **43** (New Delhi : Narosa) 406 (2000)
- [13] T Brugger, T Schreiner, G Roth, P Adelman and G Czjzek *Phys. Rev. Lett.* **71** 2481 (1993)
- [14] P Fulde *J. Low Temp. Phys.* **95** 45 (1994)
- [15] D N Zubarev *Sov. Phys. Usp.* **95** 71 (1960)
- [16] C A Balseiro and L M Falicov *Phys. Rev. Lett.* **45** 662 (1980)
- [17] R Sooryakumar and M V Klein *Phys. Rev. Lett.* **45** 66 (1980)
- [18] R Sooryakumar and M V Klein *Phys. Rev. Lett.* **B23** 3213 (2000)
- [19] G C Mohanty and S N Behera *Can. J. Phys.* **61** 1160 (1983)
- [20] G C Rout, M S Ojha and S N Behera *Int. J. Mod. Phys.* (under publication) (2002)